

Optimization-based Adaptive Assistance for Lower Limb Exoskeleton Robots with a Robotic Walker via Spatially Quantized Gait

Chaobin Zou, Zhinan Peng, Long Zhang, Fengjun Mu, *Graduate Student Member, IEEE*, Rui Huang*,
Hong Cheng, *Senior Member, IEEE*

Abstract—Gait training with human-like gait patterns can be provided by lower limb exoskeletons (LLEs) for patients with gait impairments. For patients with little effort to keep balance, using a mobile robotic walker to assist gait training with LLEs is an effective way. Since gait patterns are varying with walking speeds, it is a critical issue to coordinated control the robotic walker and the exoskeleton to obtain a natural and human-like walking posture. In this paper, a novel adaptive assistance approach named SQG-OPT is proposed to tackle the problem, which comprises of two parts: the Spatially Quantized Gait (SQG) and the optimization. The SQG generates reference joint angles and reference trajectory of the Center Of Mass (COM) for the human-exoskeleton system in space domain. The optimization part is constructed to convert the reference joint angles from the space domain to the time domain, which is based on the dynamics model of the human-exoskeleton-walker system and adaptive to different walking speeds. The proposed approach has been tested on the robot simulation platform CoppeliaSim, the experimental results indicate that the proposed approach can generate human-like gait patterns for different walking speeds from 0 to 0.8 m/s. Additionally, in comparison with other methods, the proposed approach has a better performance on the movement tracking of the COM for a natural walking posture.

Note to Practitioners—The coordinated control is important for the exoskeleton robot with a mobile robotic walker, one of the potential challenge is the adaptive coordinated motion planning for these robotic devices. The proposed approach is for the coordinated control of the exoskeleton robots with a robotic walker and adaptive to different walking speeds, which may inspires more extended coordinated control strategies for human-exoskeleton systems in more gait training applications. The proposed approach is also potential for the coordinated motion planning of the other human-centered assistance robots, such as the wheeled walking assistance robots for the elderly.

Index Terms—Exoskeleton, Robotic Walker, Spatially Quantized Gait, Optimization, Coordinated Control

I. INTRODUCTION

Robotic Lower Limb Exoskeletons (LLEs) are designed for quantified repetitive gait training for patients with gait impairments who suffer from spinal cord injury [1] [2] [3], stroke [4] [5] and cerebral palsy [6] [7]. For patients with limited muscle strength to maintain balance while gait training on the ground, using a mobile robotic walker is an effective way to support the body weight and assist them in completing gait training. As shown in Fig. 1, a patient is gait training with



Fig. 1: A patient is gait training with an exoskeleton robot associated with a robotic walker, where the weight of the human-exoskeleton system can be supported by the walker.

an exoskeleton robot and a robotic walker, where the walker is connected to the back of the exoskeleton with a cantilever, and the human-exoskeleton system can be supported by the robotic walker. On the other hand, the balance of the human-exoskeleton system can be ensured with such a robotic walker. With the assistance of the robotic walker, the exoskeleton robot can be used in gait training for most of the patients.

However, if the robotic walker can't be controlled with a compatible strategy to follow the walking of the exoskeleton robot, the gait of the human-exoskeleton system will be changed. Since the backpack of exoskeleton robot is connected to the walker, the movement of the exoskeleton robot is limited, includes but not limited to the movement of the Center Of Mass (COM), the posture of the upper body, and the gait patterns. In this paper, we focus on the problem of implementing natural walking patterns for the human-exoskeleton system with a mobile robotic walker. To the best of our knowledge, there are two challenging issues:

- For overground walking, the position of the COM is varying over time, how to implement a natural movement of COM for the human-exoskeleton system with a robotic walker to obtain a human-like walking posture?
- The gait patterns vary with the walking speed, how can the exoskeleton robot and the walker be coordinated controlled to adapt to different walking speeds?

To obtain natural gait patterns, joint angles were collected from the healthy subjects as original reference joint angles. In order to simplify the dynamics calculation of the Human-

C. Zou, Z. Peng, L. Zhang, F. Mu, R. Huang, and H. Cheng are with Center for Robotics, School of Automation Engineering, University of Electronic Science and Technology of China, 611731, Chengdu, Sichuan, P. R. China.

*R. Huang is the corresponding author. ruihuang@uestc.edu.cn

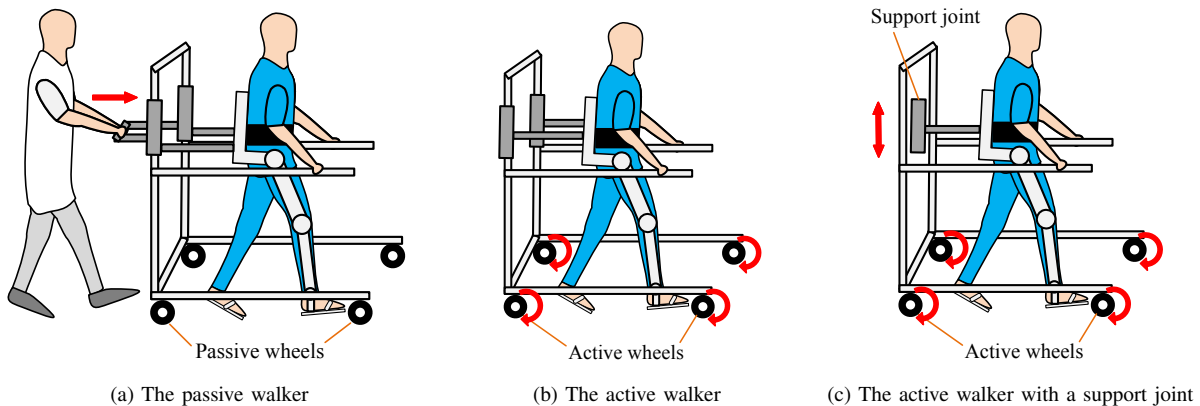


Fig. 2: Passive and active mobile robotic walkers. (a) The passive walker with passive wheels; (b) The active walker with active wheels that actuated by the DC servo motors; (c) The active walker with active wheels and a active support joint.

Exoskeleton-Walker (HEW) system, a reduced order dynamics model is employed in this paper, which can be used to model the COM's dynamic movement, and construct the optimization problem. The main contributions can be summarized as:

- A novel Spatially Quantized Gait (SQG) is proposed for human-like joint angles generation of the lower limb exoskeleton robots with a mobile robotic walker;
- By combining the dynamics model with the SQG approach, the reference joint trajectories of the robotic walker can be generated, consequently the horizontal and vertical movement assistance of the human-exoskeleton system during walking can be achieved;
- The proposed approach is adaptive to different walking speeds and offers natural walking posture assistance of the exoskeleton robots comparing with other approaches.

The remaining sections of this paper are organized as follows: In Section II, related works about the LLEs with robotic walker are presented. Section III presents the detailed explanation of the proposed approach. In Section IV, experiments are designed to evaluate the proposed approach. Conclusions and future works are given in Section V.

II. RELATED WORK

In the last decades, there were several studies on the gait training with the exoskeleton robots. There are two categories for the gait training with an external support for the human-exoskeleton system, one is the fixed frame for body weight support, and another one is the mobile robotic walker.

The fixed frames are often implemented by the body weight support systems. Lokomat is a bilateral gait orthosis for treadmill based robotic gait training [8], which provides a human-like walking posture with body weight support and a COM transfer behaviour control, as well as some impedance control based assist-as-needed control strategies [9]. Lokomat allows the patient to walk with different speeds on the treadmill. A similar device named ALEX can also provide body weight supported treadmill training for post-stroke patients [10], [11], which also allows for pelvic motion. Another similar commercially available device is the ReoAmbulator, which comprises

two actuated leg orthoses, a body weight support system and a treadmill [12]. Similar structure and control strategy can also be found on another device named LOPES, with more degree of freedom, and actuated with Bowden-cable-driven series elastic actuators [13]. Many patients benefit from these robotic gait training devices with fixed frame for body weight support and walking. However, it is not a true overground gait training. Comparing to the treadmill walking, overground walking gives more feedbacks to patients with the COM transfer and the forward stepping in real world. Therefore a mobile robotic walker is required to assist a overground gait training.

For the mobile robotic walker, there are also some studies, including the passive walker and the active walker, as shown in Fig. 2. The passive walker is with the passive wheels and with or without the exoskeleton robot legs, which requires a person to push the walker to move forward, or the walking of the patient will be affected by pulling the walker to move forward while walking. The active walker is with the active wheels and the exoskeleton robot legs, where the wheels and exoskeleton robots can be actuated by DC servo motors and both the walker and the exoskeleton robot can be controlled to move forward. There are some robotics walker for the patient's gait training without exoskeleton legs, such as the mobile robotic platform in [14] and Andago [15], they are connected to the patients with ropes and harness. These single walkers are used to support partial of the patient's body weight to reduce the burden of their legs and help them to walk with a safe environment. CPWalker is a passive robotic platform for the rehabilitation of children with cerebra palsy [16], which supports the body weight and allows the possibility of free movement of the patient to walk overground. Similar passive robotic walker with a wearable exoskeleton robots named Trexo [17] also offers facilitated and repetitive precision movement for children with gait disorders. A passive robotic walker connects to the lower limb exoskeleton named AiWalker [18] is used to evaluate the walking efficiency in the gait training of spinal cord injury patients. By using a hard connection with the waist structure of the exoskeleton robot, the weight of the patient and the exoskeleton could be

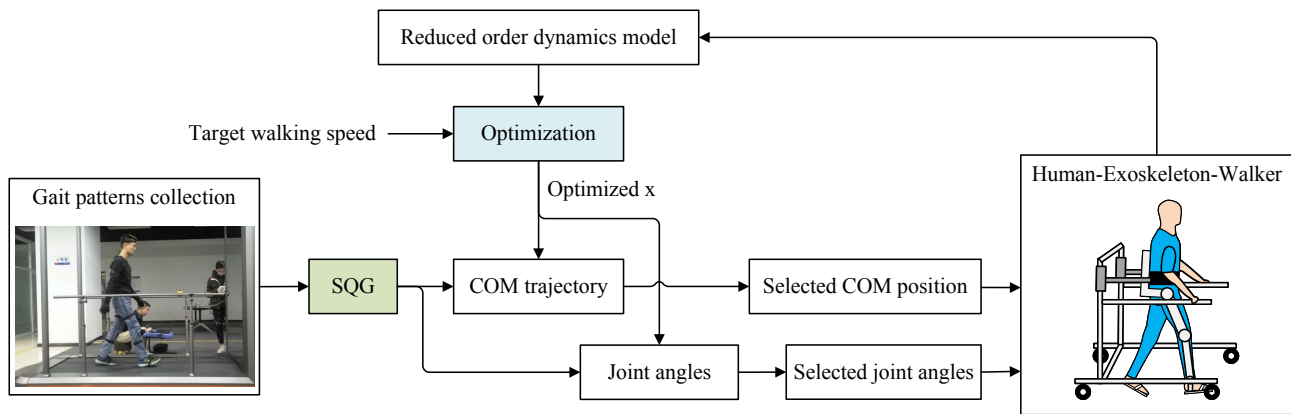


Fig. 3: The framework of the proposed SQG-OPT approach, comprises of the SQG part and the optimization part.

supported by the walker. Even the connector allows adjustable distance to fit different patients, there is no actively movement for this walker adapts to the vertical movement of the COM during walking, as shown in Fig. 2b. The coordinated control is important for not only human-robot interaction [19] but also for exoskeleton-walker system.

Overall, combining the wearable lower limb exoskeleton robots with mobile robotic walkers to provide overground gait training with true ambulation is potential for the rehabilitation of the patients. In this paper, as shown in Fig. 2c, the active robotic walker with active wheels and an active support joint is studied, which provide both the horizontal and the vertical movement assistance for the human-exoskeleton system. The main challenge is how to coordinated control the exoskeleton robot and the robotic walker to perform natural walking assistance, *i.e.*, how to generate appropriate reference joint angles for the active wheels and the support joint to follow the movement of the human-exoskeleton system. In this paper, a novel idea of Spatially Quantized Gait based optimization approach (SQG-OPT) is proposed, which aims to solve the coordinated control problem of the exoskeleton robot and the robotic walker.

III. METHODOLOGY

In this section, in order to overcome the drawbacks of the existing approaches, a novel idea of Spatially Quantized Gait (SQG) is proposed, and combined with an optimization based adaptive control framework to generate joint angles for the exoskeleton and the associated mobile robotic walker with varying walking speeds.

A. The framework of SQG-OPT

The framework of the SQG-OPT is shown in Fig. 3, which includes two main components, the SQG and the optimization. The SQG is used to generate COM's trajectories and human-like joint angles in space domain varying with the horizontal displacement x . The optimization is based on the reduced order dynamics model of the HEW system, which is used to generate optimized x as the index for the COM's position and the joint angles, *i.e.*, convert the joint angles from space domain to the time domain depends on the target walking speed. With the

selected COM's position and joint angles in time domain, the reference trajectories in time domain for the exoskeleton robot and the robotic walker can be obtained. That is the joint angles for the hip, knee and ankle joints of the exoskeleton robot, the joint angles for the support joint and the wheels of the robotic walker. After that, these joints are controlled with the PID control algorithm to track the reference joint angles.

B. Spatially Quantized Gait

Spatially Quantized Gait is inspired by the concept of Spatially Quantized Dynamics proposed in [20], [21], where the gait patterns for the biped robots are generated with the given foot locations and the kinematics calculation. However, the generated gait patterns in [20] are not human-like and not appropriate for the gait training of LLEs.

1) *Gait collection*: Compared with the calculation of the joint angles in [20], joint angles can be collected from healthy subjects with the wearable motion capture system and can be used as the original reference gait patterns of the lower limb exoskeleton robot. Since in this paper, there is only forward walking assistance with the robotic walker in Sagittal plane, *i.e.*, without lateral movement or turning, the collected joint angles are represented with the joint angles of the lower limb (hip flexion/extension, knee flexion/extension and ankle flexion/extension). In time domain, The collected joint angles can be regarded as a function of time and varying with walking speed, and can be used as the reference joint angles the lower limb exoskeleton robot to obtain the gait training with a fixed walking speed. In this paper, to obtain a varying walking speed gait training with the same collected joint angles and provide reference for the control of the robotic walker, the joint angles can be represented in space domain.

2) *Spatially quantized COM's trajectory and joint angles*: Since the movement of the COM has a good correspondence with the movement of hip joint in space domain [20], to simplify the calculation, in this paper, the COM is set to the center between two hip joints of the lower limb exoskeleton robot. Therefore, based on the collected joint angles, the COM's position during walking can be calculated and grouped as the COM's trajectory in time domain. If the COM's trajectory is spatially discretized in space domain with the horizontal

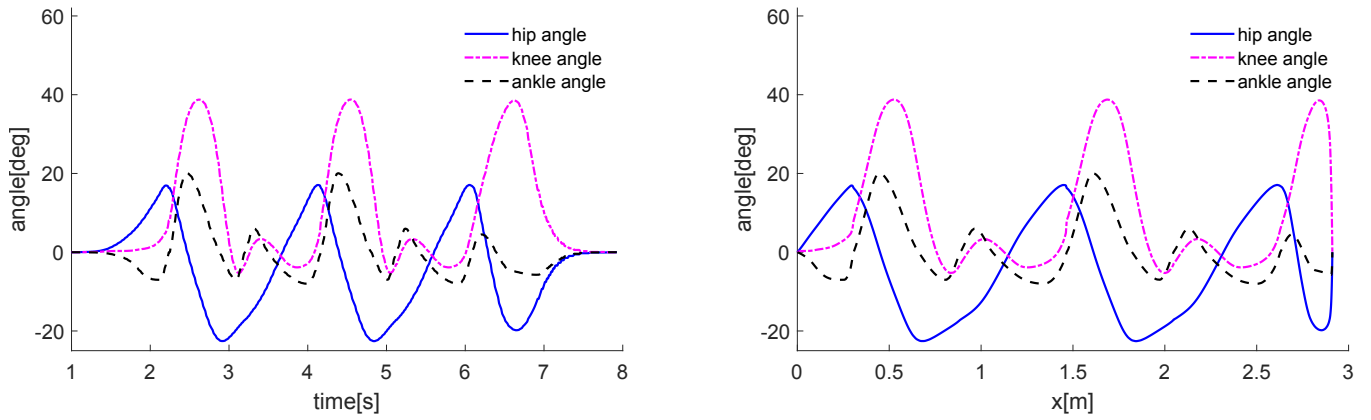


Fig. 4: The comparison of joint angles collected from the healthy subject for several steps in time domain (left) and in space domain (right), where the solid blue curve, dot dashed purple curve and dashed black curve are the hip joint angle, the knee joint angle and the ankle joint angle, respectively.

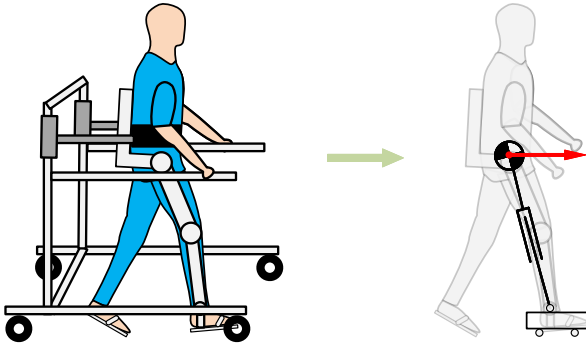


Fig. 5: The cart-pendulum model of the HEW system.

displacement of the COM by using a constant unit length Δx , e.g., $\Delta x = 0.001$ m, therefore

$$x_i = \Delta x \cdot i, \quad (1)$$

where $i = 0, 1, 2, \dots, N$ and N is the data length for several steps. Similarly, the joint angles can also be discretized in space domain with the horizontal displacement of the COM.

As shown in Fig. 4, the comparison of hip, knee and ankle joint angles in time domain and space domain are presented. Joint angles in the left figure are collected from healthy subjects in time domain, there are several steps of walking from stand posture to walk forward several steps and stop to the stand posture again. Joint angles in the right figure are same with the left figure but represented in space domain, where joint angles are varying with horizontal displacement of the COM, *i.e.*, the x . Because the horizontal movement of the COM is not a linear traveling from one position to another, there is an inner dynamic movement during walking.

In this paper, the collected joint angles with the walking speed of 0.5 m/s were selected as the original joint angles for SQG. It is possible to change the walking speed with the same collected joint angles by transferring the joint angles from time domain to space domain, *i.e.*, the walking speed can be changed to another one with the horizontal movement of the COM, and not limited to be a fixed speed associated with

the collected joint angles. In other words, the joint angles can be represented by a function of COM's horizontal movement in space domain, we call this Spatially Quantized Gait.

C. The Optimization-based Adaptive Assistance Strategy

In this subsection, the optimization based adaptive reference joint angles generation for both the lower limb exoskeleton robot and the robotic walker will be proposed. Since in the previous section, the joint angles are represented as a function of horizontal displacement of COM, now the main idea is to find an optimized x as the index for the COM's position and joint angles selection. The selected joint angles can be used to control the exoskeleton robot, and the selected COM's position can be used to control the robotic walker, thus the exoskeleton robot and the robotic walker can be coordinately controlled to adapt to different walking speeds.

1) Adaptive Walking of the Human-Exoskeleton System:

In order to obtain a natural walking posture and select the optimized x , many approach can be used. In this paper, a reduced order dynamics model has been employed to model the human-exoskeleton system. As shown in Fig. 5, regard the robotic walker's assistance as an external force for the human-exoskeleton system, then we can model the human-exoskeleton system as a cart-pendulum model, where the COM of the human-exoskeleton system is set to the center between two hip joints. The dynamics calculation of the cart-pendulum model can be represented as

$$\ddot{x} = \omega^2(x - p), \quad (2)$$

where x and \ddot{x} are horizontal displacement and acceleration of the COM, respectively. p is the ankle location, and ω is calculated as $\omega = \sqrt{g/z}$, where g is the gravity acceleration and z is the COM's height.

Refer to equation (1), the horizontal displacement of the COM has been spatially discretized with the unit length Δx . Assuming that v_i is the COM's speed corresponding to x_i , the time Δt_i for the COM travels from x_i to x_{i+1} is

$$\Delta t_i = \frac{\Delta x}{v_i}. \quad (3)$$

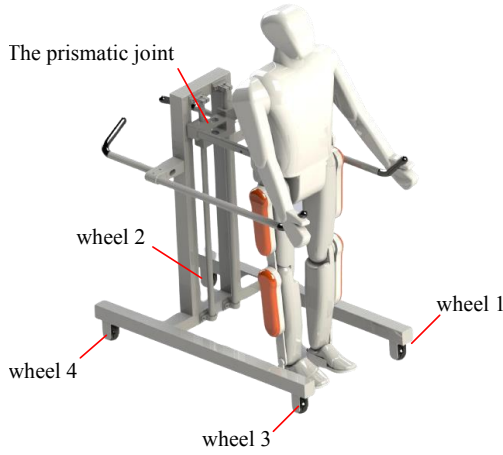


Fig. 6: The simulation model of the HEW system, including four wheels and one prismatic joint (the support joint for the vertical movement assistance) for the robotic walker.

Now we can calculate the speed of the COM at the next spatial step based on (2) as

$$\begin{aligned} v_{i+1} &= v_i + \omega^2(x_i - p_i)\Delta t_i \\ &= v_i + \omega^2(x_i - p_i)\frac{\Delta x}{v_i}, \end{aligned} \quad (4)$$

Note that v_i is the denominator in the equation, it is necessary to set a lowest value for the v_i to avoid the singularity, therefore we have

$$\|v_i\| \geq \epsilon, \quad (5)$$

where ϵ is a small positive constant value.

In order to satisfy the spatially quantized dynamics and track the references generated by SQG, we formalize an optimization problem as

$$\begin{aligned} \underset{p_i}{\text{minimize}} \quad & J := \sum_{i=1}^N (v_i - v_i^{\text{ref}})^2 + \beta (p_i - p_i^{\text{ref}})^2 \\ \text{subject to} \quad & v_{i+1} = v_i + \omega^2(x_i - p_i)\frac{\Delta x}{v_i} \\ & \|v_i\| > \epsilon \end{aligned} \quad (6)$$

where v_i^{ref} is the reference velocity profile given with the target walking speed, and p_i^{ref} is the reference ankle locations generated by SQG. β is a constant parameter. Differential Dynamic Programming (DDP) [22] was used to solve the optimization problem and find the optimized solution to equation (6). Once the optimized x_i ($i = 1, 2, 3, \dots, N$) in time space domain was found, the time for the i -th spatial data is calculated by

$$t_i = \sum_{k=1}^{i-1} \frac{\Delta x}{v_k}, \quad (7)$$

thus the joint angles and the COM's positions in time domain can be generated.

Above all, the reference gait patterns in both space domain and time domain for the target walking speed profile v_i^{ref} are generated, now let's turn to the adaptive assistance control of the robotic walker.

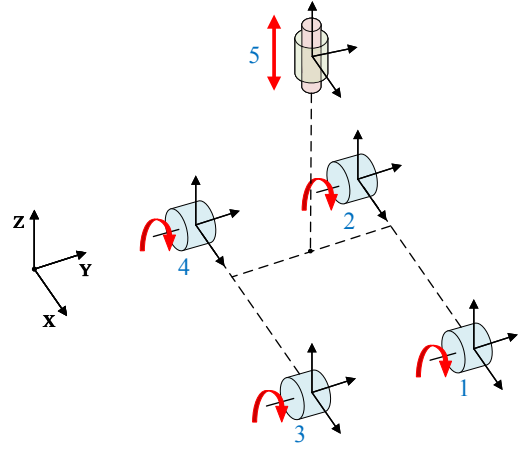


Fig. 7: The joints of the walker, where index 1 - 4 are revolute joints (around Y axis) for wheels, and 5 is the prismatic joint (along Z axis) for the vertical movement supporting.

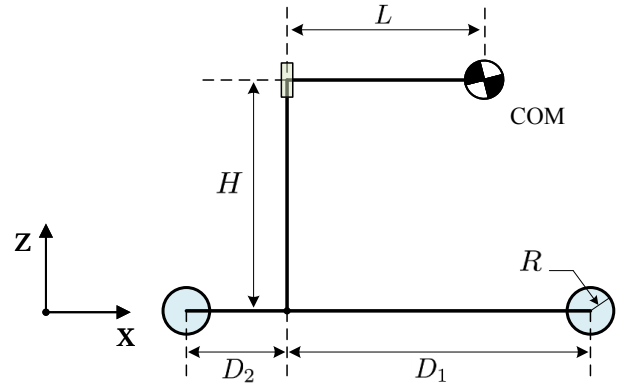


Fig. 8: The kinematic information of the robotic walker.

2) *Adaptive Assistance of the Robotic Walker*: The structure and the active joints of the walker is shown in Fig. 6, where there are four wheels and a prismatic joint on the robotic walker. The prismatic joint is connected to the backpack of the exoskeleton robot with a cantilever beam, support the some of the weight of human-exoskeleton system, and provide the vertical movement for the COM during walking.

The joints for each wheel and the prismatic joint are shown in Fig. 7, where index 1 - 4 are corresponding to wheel 1 - wheel 4 in Fig. 6, and index 5 is corresponding to the prismatic joint. For each wheel, there is a revolute joint around the Y axis, and the prismatic joint moves along the Z axis. All wheels can be set as free joint for passively movement, or actively controlled together to let the robotic walker track the human-exoskeleton walking on the ground. Note that if the wheel joints are set as free joints, the human-exoskeleton system has to pull the whole walker forward while walking. In other words, the robotic walker gives an external force to pull the human-exoskeleton back while walking forward, which has a bad effects for human-exoskeleton walking. If the wheel joints are actively controlled and let the robotic walker to track the movement of the human-exoskeleton system, then an appropriate tracking reference for the wheels are required,

in other words, target reference joint angles are required, especially with different walking speeds. We will compare the performance for both passive wheel joints and active wheel joints in the section IV, and we will find that the active assistance of the robotic walker is necessary for the natural walking of the human-exoskeleton system.

In section III-B2, the COM's trajectory in space domain has been generated and is adaptive to different walking speeds. In order to track the vertical and horizontal movement of the COM, the kinematic relationship among the prismatic joint, wheel joints and the COM should be known. As shown in Fig. 8, the kinematics size of all joints on the robotic walker is illustrated, where H is the relative height between prismatic joint and the wheel center, L is the relative distance between the prismatic joint and the COM, R is the radius of the wheel, D_1 is relative horizontal distance between prismatic joint and front wheels (wheel 1 and wheel 3), and D_2 is relative horizontal distance between prismatic joint and back wheels (wheel 2 and wheel 4). Assuming that the position of COM is represented by

$$P_{COM} = [x, y, z]^T, \quad (8)$$

then the position of the prismatic joint can be calculated as follows:

$$P_{pj} = P_{COM} + [-L, 0, 0]^T, \quad (9)$$

which means the vertical position of the prismatic joint is varying with the position of the COM simultaneously, the vertical position of the prismatic joint should be same with the COM. The joint positions of wheels can be calculated as

$$\begin{cases} P_{w1} = P_{COM} + [D_1 - L, W/2, -H - R]^T \\ P_{w2} = P_{COM} + [-D_2 - L, W/2, -H - R]^T \\ P_{w3} = P_{COM} + [D_1 - L, -W/2, -H - R]^T \\ P_{w4} = P_{COM} + [-D_2 - L, -W/2, -H - R]^T \end{cases} \quad (10)$$

where $P_{w1}, P_{w2}, P_{w3}, P_{w4}$ are positions for the wheel joint 1 to wheel joint 4, respectively. W is the width of the walker, *i.e.*, relative distance between two front wheels. In section III-B2, the COM's trajectory is spatially discretized in space domain with a small displacement Δx , in the same way, the joint angles for wheels can also be spatially discretized in space domain with a small angle change, which is calculated as

$$\Delta\theta = \frac{\Delta x}{R}. \quad (11)$$

Now, we can generate the reference joint angles for robotic walker's wheels based on the COM's reference trajectory in space domain.

Above all, the reference trajectories of COM, prismatic joint and wheel joints can be generated based on the collected joint angles from healthy subjects and the target walking speed. In the following section, the effectiveness of the proposed method will be verified in comparison with other methods.

IV. EXPERIMENTAL RESULTS AND DISCUSSION

In this section, experiments are designed to evaluate the proposed approach on the robot simulation platform named

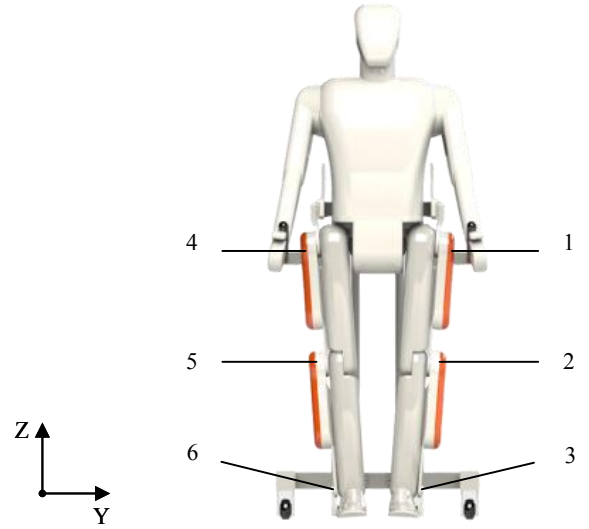


Fig. 9: The simulation model of the HEW system in the front view. 1: the left hip joint, 2: the left knee joint, 3: the left ankle joint, 4: the right hip joint, 5: the right knee joint, 6: the right ankle joint.

CoppeliaSim¹. In comparison with the other non-adaptive assistance approaches of the robotic walker, the proposed approach has a better performance on the COM's movement tracking and human-like gait patterns generation for the natural walking posture. In addition to this, the proposed approach is adaptive to different walking speeds from 0 to 0.8 m/s in the experiment.

A. The experiment setup

The simulation model of the robotic walker is shown in Fig. 6, including one prismatic joint and four wheel joints. The simulation model of the exoskeleton robot is shown in Fig. 9, including six revolute joints (flexion/extension) for hip, knee, and ankle joints, respectively. There is a humanoid dummy to simulate the patient with gait disorders, where the lower limbs of the dummy are banded to the exoskeleton's leg, all joints of the dummy are passive to simulate a paraplegic patient. Additionally, reference to the real HEW system shown in Fig. 1, the weight of the humanoid dummy, the exoskeleton robot and the robotic walker are set to 60 kg, 20 kg and 80 kg, respectively. Note that in this paper, we focus on the movement in the Sagittal plane, therefore all joints of the exoskeleton's leg revolve around the Y axis for the flexion and extension movement. The joints of the simulation model are controlled in the position mode with PID joint controllers.

As mentioned in section II, some existing robotic walkers are passive walkers to follow the walking of the human-exoskeleton system, and other robotic walkers are actively controlled to assist the walking of the human-exoskeleton system with non-adaptive control strategies. Therefore in this paper, three different assistance strategies for the robotic walker are designed for the comparison, passive assistance of

¹<https://www.coppeliarobotics.com>

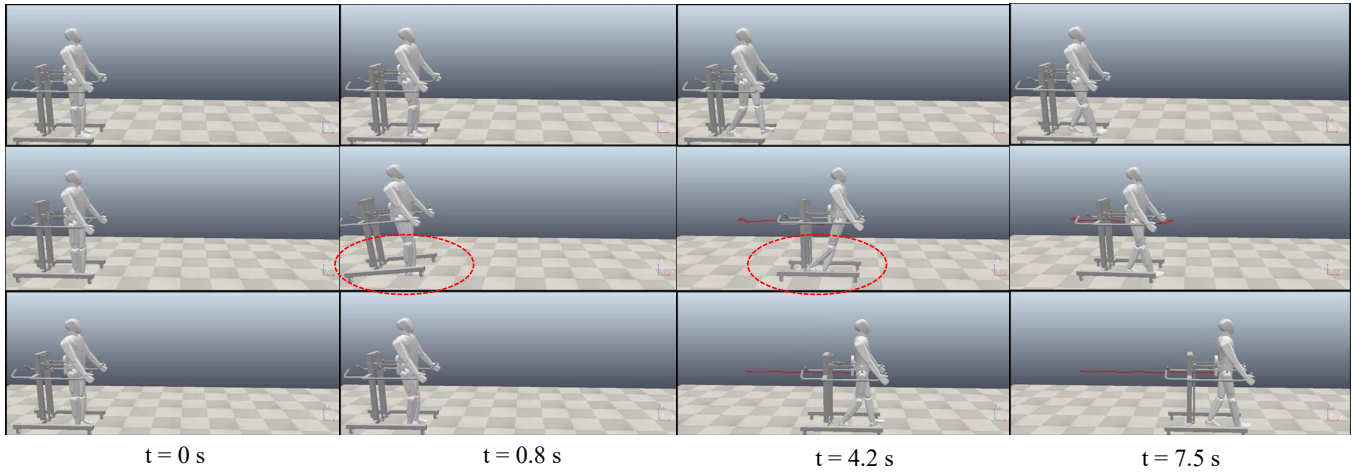


Fig. 10: The simulation snapshots of PA. The comparison of walking with different COM's heights is shown, where the top row of figures are with a higher position than the required COM's height, the middle row of figures are with a lower position than the required COM's height, and the bottom row of figures are with the position closed to the required COM's height.

the walker, non-adaptive active assistance of the walker, and adaptive active assistance of the walker. Additionally, three different walking speeds (0.3 m/s, 0.5 m/s and 0.8 m/s) are designed in the experiments to evaluate the adaption of the proposed approach. Some parameters in previous equations are set as constant values, e.g., z is set to the mean height of the COM, $g = 9.81 \text{ m/s}^2$, $\beta = 1.0$, $\epsilon = 0.001 \text{ m/s}$.

1) *Passive assistance of the walker (PA)*: In this case, in order to finish the overground gait training, the weight of human-exoskeleton system is supported by the robotic walker, *i.e.*, the prismatic joint should be set to a fixed position based on the height of the COM. The wheel joints of the robotic walker are set to be passive and free to roll over the ground. As a result, the human-exoskeleton system has to pull the robotic walker forward during walking.

2) *Nonadaptive active assistance of the walker (NA)*: In this case, the wheel joints of the robotic walker are controlled with PID joint controllers. A fixed rolling speed is set for the wheels due to the lack of control reference. However, it is a challenge to set an appropriate rolling speed for the wheels to follow up the walking of the human-exoskeleton system, a faster or slower speed always leads to problems.

3) *Adaptive active assistance of the walker (AA)*: The SQG-OPT is used in the experiment of adaptive active assistance of the HEW system. The Biped Robot Gait (BRG) generation strategy with the stretch knee constraint proposed in [20] is adopt for the comparison with SQG-OPT. Additionally, the joints of the walker are controlled with PID joint controllers to track the reference trajectories generated by the SQG-OPT and BRG.

B. The simulation experiments

In the following paragraphs, the simulation experiments of PA, NA, and AA are presented. Note that the corresponding video could be found here².

The simulation snapshots of PA are shown in Fig. 10. In this case, the wheels of the robotic walker are free to move with no active control, and the prismatic joint is set to a fixed position for the weight support of human-exoskeleton system, which leads to the walking with no vertical movement of COM. Since the required COM's height during walking is unknown, the only way to set the position of the prismatic joint is to try different settings by trail and error, which is time consuming and may leads to a bad performance. For the top row of figures in Fig. 10, if the position of the prismatic joint is set to a higher position than the required COM's height, the human-exoskeleton system is hang-up during walking with the feet off the ground, which is not a true overground gait training. For the middle row of figures in Fig. 10, if the position of the prismatic joint is set to a lower position than the required COM's height, the robotic walker will be lifted during walking. As shown in the red circle of the second and the third picture, there is a potential risk of falling down. For the bottom row of figures in Fig. 10, after several trails, if the position of the prismatic joint can be set to a position that is closed to the required COM's height, the HEW system can be controlled to walk forward normally. However there is no vertical movement of the COM, which is not a natural walking posture of the human-exoskeleton system.

The simulation snapshots of NA with different moving speeds is shown in Fig. 11, where the top, middle, and bottom rows of figures are with the fixed moving speed of 0.3 m/s, 0.5 m/s and 0.8 m/s for the robotic walker, respectively. With actively controlled wheel joints, the human-exoskeleton system will be pushed forward with the robotic walker, as a result, the walking speed of the HEW system is determined by the moving speed of the robotic walker. However, the moving speed of the robotic walker may not be coordinated with the walking speed of the human-exoskeleton system. The human-exoskeleton system will be pull back during walking with a lower moving speed. On the contrary, the human-exoskeleton system will be pushed forward with a higher moving speed,

²<https://www.youtube.com/watch?v=t2-vMH27874>

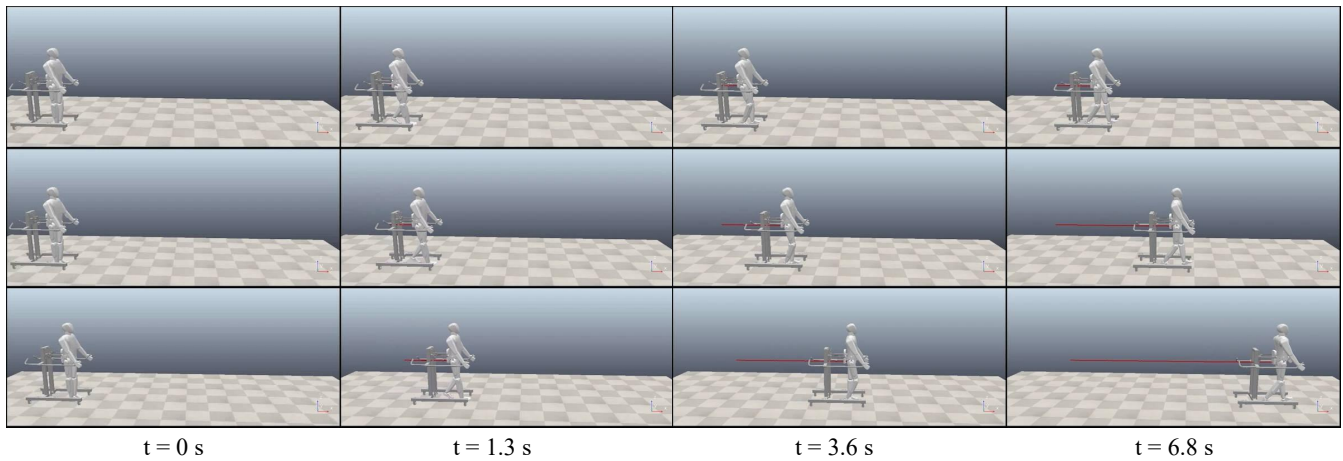


Fig. 11: The simulation snapshots of NA with different fixed moving speeds for the robotic walker, where the top row of figures are with 0.3 m/s, the bottom row of figures are with 0.8 m/s, and the middle row of figures are with 0.5 m/s.

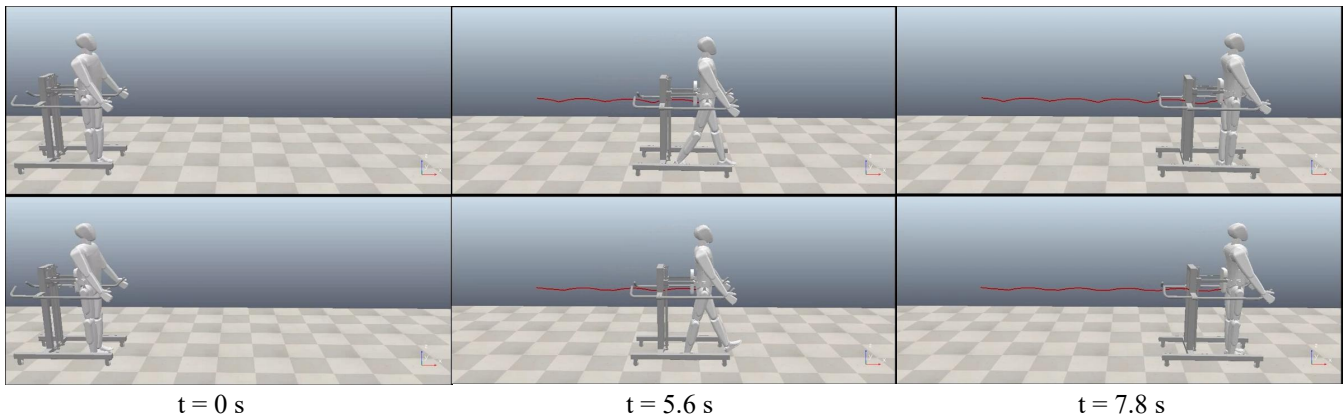


Fig. 12: The simulation snapshots of AA, where the top row of figures are with the joint angles generated by BRG, and the bottom row of figures are with the joint angles generated by SQG.

it looks like the human-exoskeleton is drifting overground, not walking overground. On the other hand, similar to the cases in Fig. 10, there is also no vertical movement of the COM. Mismatched moving speed with no vertical movement of the COM leads to an unnatural and not human-like walking posture, and leads to bad gait training for patients in extreme cases. Therefore, an adaptive and coordinate control approach for human-exoskeleton system with a robotic walker is necessary.

The simulation snapshots of AA with the walking speed of 0.5 m/s and two different gait patterns generation method by SQG and BRG are shown in Fig. 12, where the top row of figures are with joint angles generated by BRG, and the bottom rows of figure are with joint angles generated by SQG, respectively. The HEW system is controlled to produce a normal walking posture with both BRG and SQG approach, there are different performance on the tracking of the COM's movement and the joint angle generations. In addition to this, the comparison of these two approaches will be discussed in the following subsections.

C. The experimental results

In order to evaluate the effectiveness of the proposed approach, experimental data were collected and analyzed in the following paragraphs. To evaluate the coordination between the human-exoskeleton system and the robotic walker, the COM's movement tracking performance during walking is presented. On the other hand, to evaluate the adaption of the proposed approach for different walking speeds, the joint angles generation and tracking results for both the exoskeleton robots and the robotic walker are presented.

1) *The COM's movement tracking performance:* The COM's reference trajectories generated by SQG and the COM's actual trajectories collected from the simulation platform with different approaches are shown in Fig. 13. The comparison of the NA and AA as well as the comparison of the SQG and BRG approaches are discussed in the following two paragraphs.

Firstly, the comparison of the COM's trajectory tracking with nonadaptive assistance of the walker (*i.e.* NA) and adaptive assistance of the walker (*i.e.* AA) is shown in Fig. 13a. The solid purple curve is the COM's reference trajectory during walking calculated with SQG, the dashed blue curve

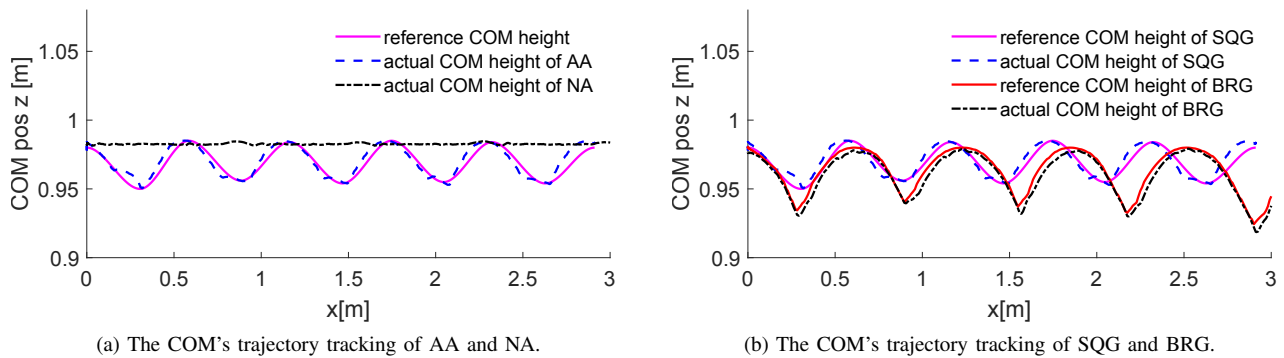


Fig. 13: The COM's trajectory generation and tracking performance during walking in the CoppeliaSim.

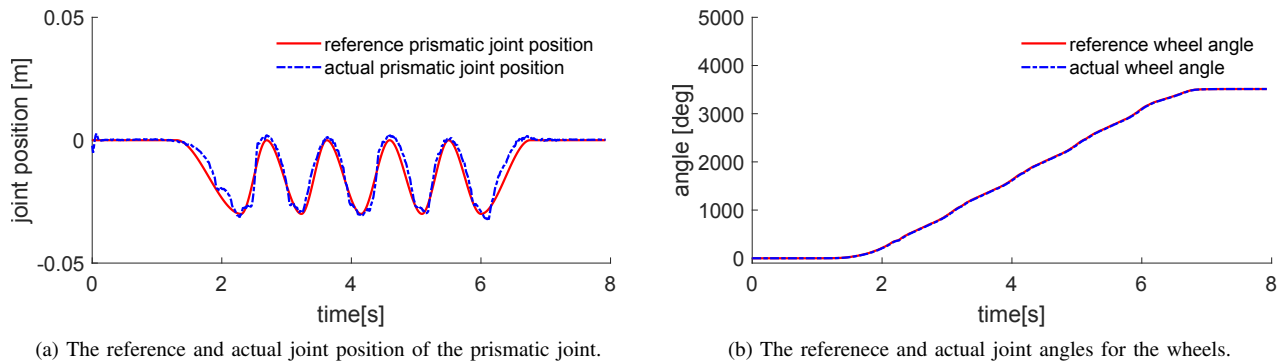


Fig. 14: The joint position/angles tracking performance of the prismatic joint and the wheels during walking in the CoppeliaSim.

and dashed black curve are the COM's actual trajectories collected from the simulation platform in AA case and NA case, respectively. In NA case, there is no vertical movement of the COM, so the COM's actual height keeps nearly constant during walking. In AA case, with the active assistance of the prismatic joint, there is vertical movement for the COM to track the COM's reference trajectory, and the COM's actual height is varying naturally along with the reference trajectory during walking. From attached video, we could also find that with prismatic joint's adaptive position control, the walking posture is more natural than the nonadaptive case.

Secondly, the comparison for AA case with different gait generation approaches by SQG and BRG is shown in Fig. 13b. The solid purple curve is the COM's reference trajectory generated with SQG, the dashed blue curve is the COM's actual trajectory collected from the simulation platform with SQG strategy. The solid red curve is the COM's reference trajectory generated with BRG, the dashed black curve is the COM's actual trajectory collected from the simulation platform with BRG strategy. The COM's reference trajectory of SQG is calculated with the collected joint angles from the healthy subjects, which has a good correspondence to the movement of the COM. The COM's reference trajectory of BRG is calculated from the artificial stepping positions with the constraint of knee stretch [20], which is not result in a natural movement of the COM and leads to more tracking errors of the COM's movement. The Mean Absolute Error (MAE) of the COM's trajectories tracking in Fig. 13 is shown in Table I, there are very small tracking errors for the AA case and more errors in other cases. Therefore the COM's

TABLE I: The MAE of the COM's trajectory tracking.

Group	AA	NA	BRG
MAE	0.0006 m	0.0286 m	0.0359 m

movement with SQG is more humanlike and closed to the natural movement during walking and can be used as the control reference of the human-exoskeleton system for the walking on the level ground.

Lastly, to implement the COM's tracking performance in Fig. 13a for AA, the reference and the actual prismatic joint positions in time domain are shown in Fig. 14a, note that the initial joint position of prismatic joint is set to zero when the prismatic joint has a same height with the COM at the beginning, *i.e.*, with the standing upright posture of the human-exoskeleton system. In addition, the reference and the actual joint angles for wheels in time domain are shown in Fig. 14b, note that in order to implement a forward overground moving without turning, the reference and actual joint angles should be same for all wheels.

2) *Joint angles generation*: Except for the COM's trajectory generation, reference joint angles should also be generated with SQG and BRG approach for the control of the exoskeleton robot. SQG and BRG both generate reference joint angles in space domain and time domain, as shown in Fig. 15, where the left column of figures are hip, knee and ankle joint angles in space domain, and the right column of figures are hip, knee and ankle joint angles in time domain. Note that the joint

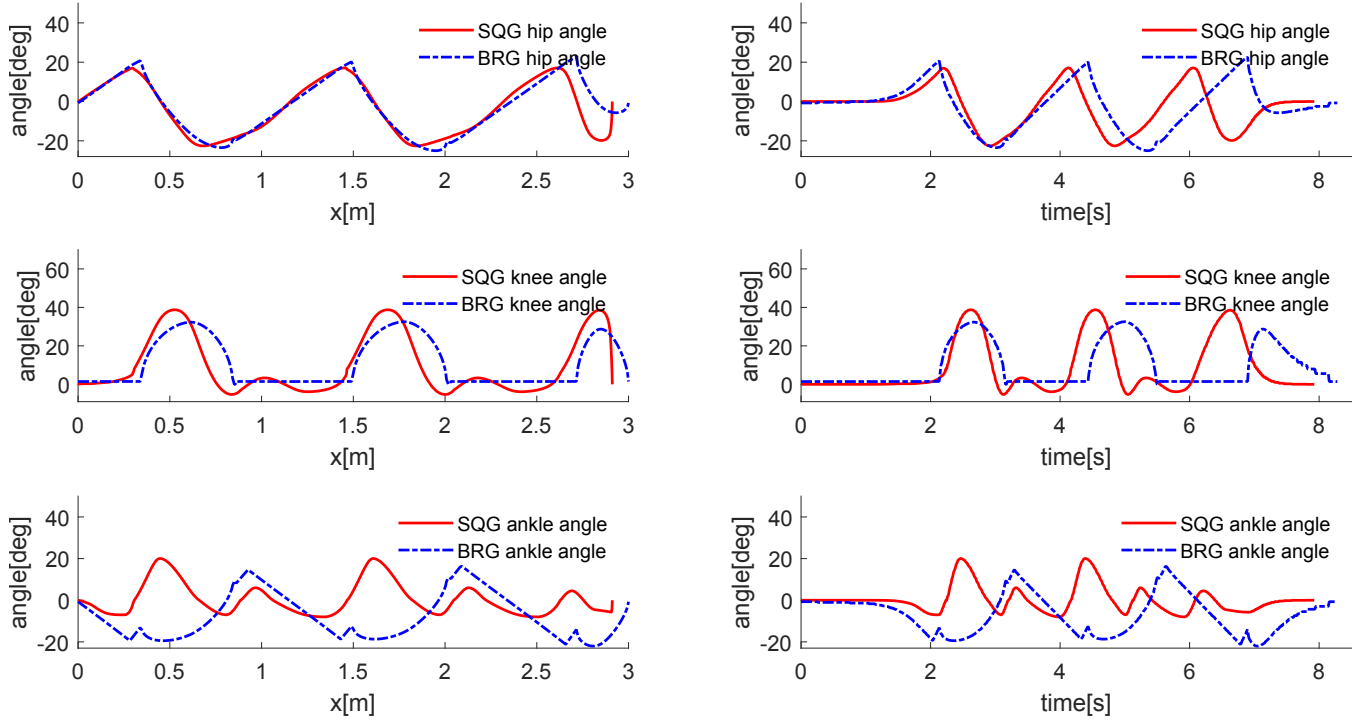


Fig. 15: The joint angles generated by SQG and BRG in space domain (left column) and in time domain (right column).

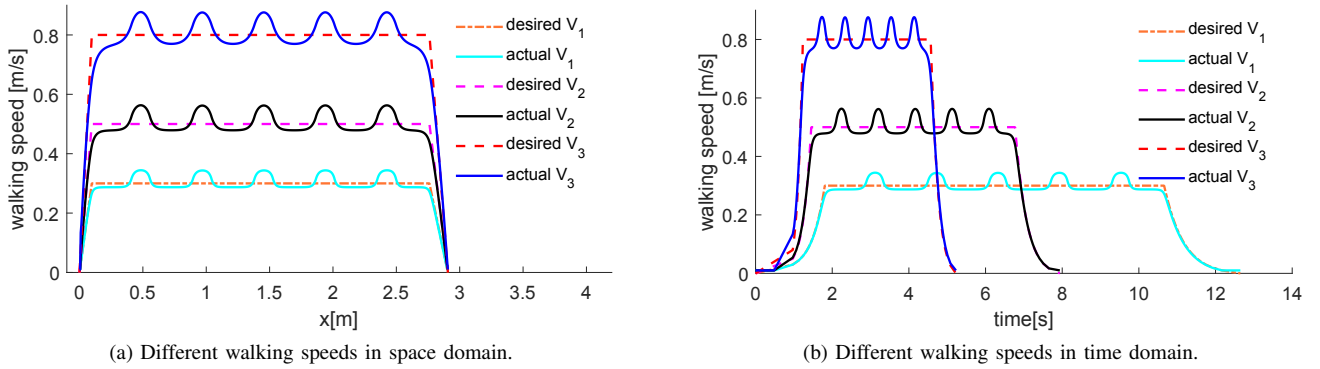


Fig. 16: The comparison of different target walking speeds, where $V_1 = 0.3$ m/s, $V_2 = 0.5$ m/s, $V_3 = 0.8$ m/s. The dashed trajectories are desired walking speeds, and the solid trajectories are actual walking speeds generated by the optimization.

angles generated by SQG and BRG in time domain are with the walking speed of 0.5 m/s. For the hip joint angles, the joint angles generated by BRG are very closed to the joint angles generated by SQG in space domain, but there is a big margin between them in time domain. For the knee and ankle joint angles, there are huge differences between BRG and SQG in both the space domain and the time domain. Since the joint angles generated by SQG are based on the collected joint angles from the healthy subjects, they are raw natural and human-like for the lower limb exoskeleton robot as the reference joint angles.

Although the reference joint angles generated by BRG also lead to the vertical movement of the COM, the walking posture is mechanical and not human-like, please refer to the attached video for the unnatural behaviours of the human-exoskeleton system with BRG during walking. For instance, the knee joint goes to the stretch joint angle and keeps constant for late swing

gait phase and the whole support gait phase, which leads to a rigid touch with the ground and looks mechanical.

From above two subsections, reference prismatic joint position and wheel angles can be generated with SQG-OPT in both space domain and time domain. Comparing to the similar approach BRG, the horizontal and vertical movement of the COM with SQG can be more natural and closed to the ground truth. As a result, the coordinated control of the human-exoskeleton system and the robotic walker can be achieved. In addition, the joint angles generated by SQG are more human-like and lead to a natural walking posture of human-exoskeleton-walker system.

3) *Adaption to different walking speeds:* Except for generating references for the walking speed associated with the collected joint angles, SQG is adaptive to different walking speeds according to the optimization in equation (6). As shown in Fig. 16, note that the original walking speed is $V_2 = 0.5$ m/s,

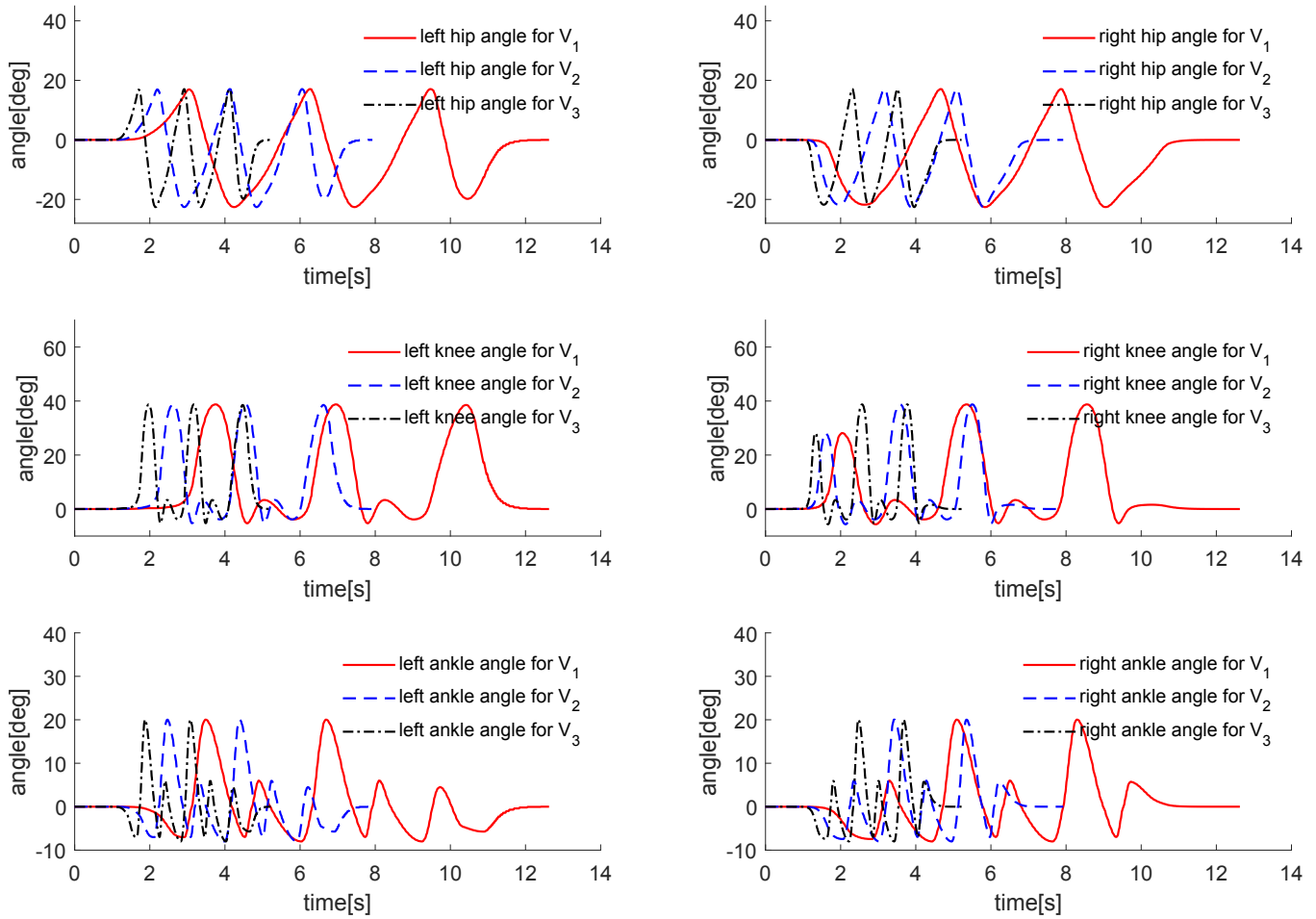


Fig. 17: The joint angles for different walking speeds, where $V_1 = 0.3 \text{ m/s}$, $V_2 = 0.5 \text{ m/s}$ and $V_3 = 0.8 \text{ m/s}$, respectively.

given a lower desired walking speed $V_1 = 0.3 \text{ m/s}$ and a higher desired walking speed $V_3 = 0.8 \text{ m/s}$, the actual walking speed in space domain and time domain can be generated with the dynamics of cart-pendulum model as the constraint. In other words, SQG-OPT can be regarded as a time-scaling human-like joint angles generation strategy to satisfy dynamic constraints. As a result, the HEW system is dynamically applicable in gait training with different walking speeds.

Given different target walking speeds, the corresponding reference joint angles for the prismatic joint, the wheel joints, and exoskeleton robot's joints in both the space domain and time domain can be generated. As shown in Fig. 17, based on the joint angles generated by SQG in the space domain and the optimized x of the COM with different walking speeds, the hip, knee and ankle joint angles are generated in the time domain. The dashed black curves, the dashed blue curves, and the solid red curves are for $V_1 = 0.3 \text{ m/s}$, $V_2 = 0.5 \text{ m/s}$ and $V_3 = 0.8 \text{ m/s}$, respectively. In other words, the time-scaled joint angles adapt to different walking speeds is generated by SQG-OPT approach. The simulation snapshots of the HEW system with different walking speeds are shown in Fig. 18, where the top row of figures are with the walking speed V_1 , the middle row of figures are with the walking speed V_2 , and the bottom row of figures are with the walking speed

V_3 , respectively. In comparison with the walking with V_2 , walking with V_1 and V_3 are with same foot locations and COM's movements but different stepping frequencies. Finally, the HEW system reached the same positions in all cases but with different durations. For a direct visualization of the experiments, please refer to the video³ recorded from the simulation experiments.

D. Discussion and limitations

According to the experimental results, we could find that the proposed approach could generate adaptive references for the coordinated control the HEW system, including joint angles for the exoskeleton robot and the robotic walker. Although the generated joint angles are adaptive to different walking speeds, it can not adapt to different patients with different anthropometric parameters online, because the raw joint angles for SQG are fixed and collected from the healthy subjects. In order to generate individualized gait patterns for different patients, SQG-OPT can be combined with other gait pattern generation approaches such as the Fourier series based approach [23] or our previous work [24].

On the other hand, there is no lateral movement assistance for COM's transfer in the frontal plane, because there is no

³<https://www.youtube.com/watch?v=t2-vMH27874>

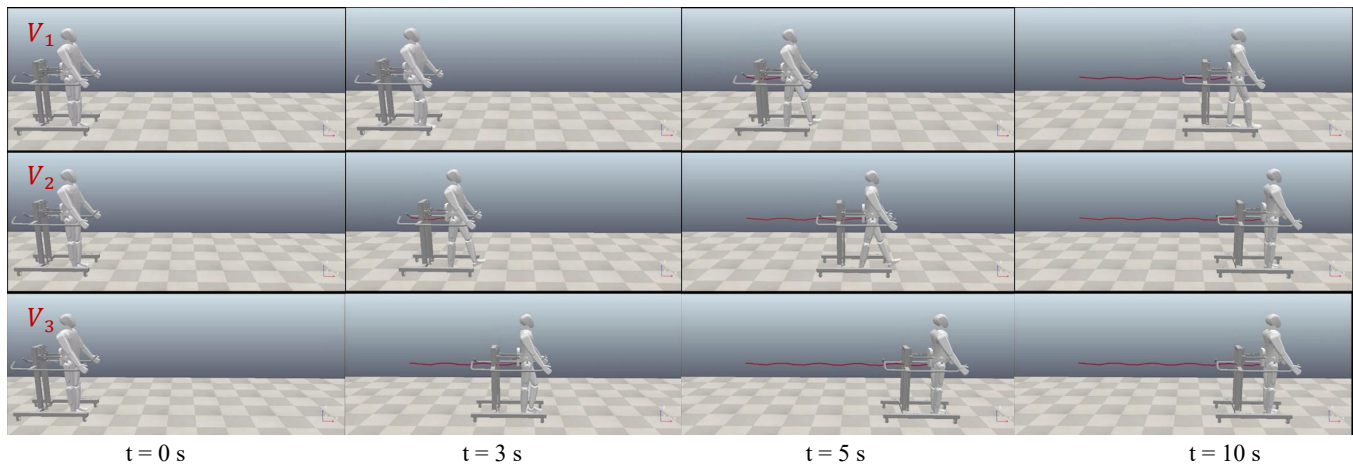


Fig. 18: The simulation snapshots of walking with joint angles generated by SQG-OPT for different desired walking speeds.

more joints to provide the lateral movement for the whole HEW system. But don't worry about it, the lateral movement is independent of the movement in the Sagittal plane, if there are more joints in the HEW system (e.g., the external/internal rotation joints for the hip joints of the exoskeleton robot, the eversion/inversion joints for the ankle joints of the exoskeleton robot, and the universal joints of the robotic walker's wheels), the simplest way to offer a balanced walking assistance is employing another approach to generate lateral movement in the front plane, such as the zero moment point based balanced walking patterns generation [25].

V. CONCLUSION AND FUTURE WORK

In this paper, we proposed an adaptive assistance approach named SQG-OPT for the lower limb exoskeleton with a mobile robotic walker, which generate coordinated motion for the adaptive control of the human-exoskeleton-walker system for varying walking speeds. The main idea is to transfer the collected joint angles from the time domain to the space domain, and calculate the corresponding COM's trajectory for the vertical and horizontal movement as well as the stepping locations in the space domain, we call this SQG. By modeling the human-exoskeleton system as a cart-pendulum model, an optimization problem could be constructed to find the optimal COM's locations with different desired walking speeds from 0 to 0.8 m/s and generate the corresponding joint angles. Compared with the passive robotic walker and nonadaptive assistance control strategy, the proposed adaptive assistance strategy provide the coordinated control references for the human-exoskeleton system and the robotic walker to walk naturally with the appropriate assistance for the COM's movement. In addition, compared with the calculated gait patterns in other studies, gait patterns generated by the SQG-OPT are more human-like and appropriate for overground gait training.

In future work, extending the SQG-OPT to be more robust for individualized gait training is a potential research topic. For instance, combined with the movement primitives based gait generation approaches or personalized gait patterns prediction approaches for patients with different anthropometric

parameters, combined with some balanced motion planning and control approaches for different terrains.

ACKNOWLEDGMENT

This work was supported in part by the National Key Research and Development Program of China (No. 2018AAA0102504); in part by the National Natural Science Foundation of China (NSFC) (No. 62003073, No. 62203089, No. 62303092); in part by the Sichuan Science and Technology Program (2022NSFSC0890, 2021YFS0383, 2023YFG0024, 2022YFS0570, 2022NSFSC0865); in part by the Fundamental Research Funds for the Central Universities (ZYGX2022YGRH003, ZYGX2021YGLH003).

REFERENCES

- [1] L. E. Miller, A. K. Zimmermann, and W. G. Herbert, "Clinical effectiveness and safety of powered exoskeleton-assisted walking in patients with spinal cord injury: systematic review with meta-analysis," *Medical Devices*, vol. 9, p. 455, 2016.
- [2] Y. Ma, X. Wu, S. X. Yang, C. Dang, D.-X. Liu, C. Wang, C. Wang, and C. Chen, "Online gait planning of lower-limb exoskeleton robot for paraplegic rehabilitation considering weight transfer process," *IEEE Transactions on Automation Science and Engineering*, vol. 18, no. 2, pp. 414–425, 2021.
- [3] C. Zou, R. Huang, J. Qiu, Q. Chen, and H. Cheng, "Slope gradient adaptive gait planning for walking assistance lower limb exoskeletons," *IEEE Transactions on Automation Science and Engineering*, vol. 18, no. 2, pp. 405–413, 2021.
- [4] J. Vaughan-Graham, D. Brooks, and L. e. a. Rose, "Exoskeleton use in post-stroke gait rehabilitation: a qualitative study of the perspectives of persons post-stroke and physiotherapists," *Journal of NeuroEngineering and Rehabilitation*, vol. 17, no. 1, pp. 1–15, 2020.
- [5] V. Longatelli, A. Pedrocchi, E. Guanziroli, F. Molteni, and M. Gandolla, "Robotic exoskeleton gait training in stroke: An electromyography-based evaluation," *Frontiers in Neurobotics*, vol. 15, p. 733738, 2021.
- [6] Z. F. Lerner, D. L. Damiano, and T. C. Bulea, "A lower-extremity exoskeleton improves knee extension in children with crouch gait from cerebral palsy," *Science translational medicine*, vol. 9, no. 404, p. eaam9145, 2017.
- [7] B. C. Conner, N. M. Remec, E. K. Orum, E. M. Frank, and Z. F. Lerner, "Wearable adaptive resistance training improves ankle strength, walking efficiency and mobility in cerebral palsy: A pilot clinical trial," *IEEE Open Journal of Engineering in Medicine and Biology*, vol. 1, pp. 282–289, 2020.
- [8] S. Jezernik, G. Colombo, and M. Morari, "Automatic gait-pattern adaptation algorithms for rehabilitation with a 4-dof robotic orthosis," *IEEE Transactions on Robotics & Automation*, vol. 20, no. 3, pp. 574–582, 2004.

- [9] A. Duschau-Wicke, J. von Zitzewitz, A. Caprez, L. Lunenburger, and R. Riener, "Path control: A method for patient-cooperative robot-aided gait rehabilitation," *IEEE Transactions on Neural Systems and Rehabilitation Engineering*, vol. 18, no. 1, pp. 38–48, 2010.
- [10] S. K. Banala, S. K. Agrawal, S. H. Kim, and J. P. Scholz, "Novel gait adaptation and neuromotor training results using an active leg exoskeleton," *IEEE/ASME Transactions on Mechatronics*, vol. 15, no. 2, pp. 216–225, 2010.
- [11] S. Shraddha, K. Pei, Chun, S. R. Darcy, P. S. John, K. A. Sunil, and S. H. Jill, "Robotic assist-as-needed as an alternative to therapist-assisted gait rehabilitation," *International Journal of Physical Medicine & Rehabilitation*, vol. 4, no. 5, pp. 370 – 378, 2016.
- [12] West RG. Powered gait orthosis and method of utilizing same. US6689075 B2, Feb. 10, 2004.
- [13] J. F. Veneman, R. Kruidhof, E. E. G. Hekman, R. Ekkelenkamp, E. H. F. Van Asseldonk, and H. Van Der Kooij, "Design and evaluation of the Lopes exoskeleton robot for interactive gait rehabilitation," *IEEE Transactions on Neural Systems and Rehabilitation Engineering*, vol. 15, no. 3, pp. 379 – 386, 2007.
- [14] G. Aguirre-Ollinger, A. Narayan, F. A. Reyes, H.-J. Cheng, and H. Yu, "An integrated robotic mobile platform and functional electrical stimulation system for gait rehabilitation post-stroke," in *Converging Clinical and Engineering Research on Neurorehabilitation III*. Cham: Springer International Publishing, 2019, pp. 425–429.
- [15] M. Detlef, S. Raoul, D. Alexander, H. Tommy, P. P. Liliana, Z. Daniel, and C. M. Jens, "The andago for overground gait training in patients with gait disorders after stroke - results from a usability study," *Physiotherapy Research and Reports*, vol. 3, no. 1, pp. 1 – 8, 2019.
- [16] F. A. Luis, A. C. Carlos, M. Marcela, B. Cristina, R. Oscar, L. Sergio, F. Anselmo, and R. Eduardo, "Evaluation of biomechanical gait parameters of patients with cerebral palsy at three different levels of gait assistance using the cpwalker," *Journal of NeuroEngineering and Rehabilitation*, vol. 16, no. 15, pp. 195 – 204, 2019.
- [17] D. Christa, M., T. Robyn, L., R. Liliane, W. James, G., and C. Elizabeth, G., "Robotic lower extremity exoskeleton use in a non-ambulatory child with cerebral palsy: a case study," *Disability and Rehabilitation: Assistive Technology*, vol. 18, no. 5, pp. 497–501, 2023.
- [18] S. Chen, Z. Wang, Y. Li, J. Tang, X. Wang, L. Huang, Z. Fang, T. Xu, J. Xu, F. Guo, Y. Wang, J. Long, X. Wang, F. Liu, J. Luo, Y. Wang, X. Huang, Z. Jia, M. Shuai, and J. Li, "Safety and feasibility of a novel exoskeleton for locomotor rehabilitation of subjects with spinal cord injury: A prospective, multi-center, and cross-over clinical trial," *Frontiers in Neurorobotics*, vol. 16, p. 848443, 2022.
- [19] X. Liu, W. Jiang, H. Su, W. Qi, and S. S. Ge, "A control strategy of robot eye-head coordinated gaze behavior achieved for minimized neural transmission noise," *IEEE/ASME Transactions on Mechatronics*, vol. 28, no. 2, pp. 956–966, 2023.
- [20] S. Kajita, M. Benallegue, R. Cisneros, T. Sakaguchi, S. Nakaoka, M. Morisawa, K. Kaneko, and F. Kanehiro, "Biped walking pattern generation based on spatially quantized dynamics," in *2017 IEEE-RAS 17th International Conference on Humanoid Robotics (Humanoids)*, 2017, pp. 599–605.
- [21] Y. Onishi, S. Kajita, T. Ibuki, and M. Sampei, "Knee-stretched biped gait generation along spatially quantized curves," in *2021 IEEE/RSJ International Conference on Intelligent Robots and Systems (IROS)*, 2021, pp. 5120–5127.
- [22] Y. Tassa, N. Mansard, and E. Todorov, "Control-limited differential dynamic programming," in *2014 IEEE International Conference on Robotics and Automation (ICRA)*, 2014, pp. 1168–1175.
- [23] S. Y. Shin and J. Sulzer, "An online transition of speed-dependent reference joint trajectories for robotic gait training," in *2019 IEEE 16th International Conference on Rehabilitation Robotics (ICORR)*, 2019, pp. 983–987.
- [24] C. Zou, R. Huang, H. Cheng, and J. Qiu, "Learning gait models with varying walking speeds," *IEEE Robotics and Automation Letters*, vol. 6, no. 1, pp. 183–190, 2021.
- [25] M. Li, T. Aoyama, and Y. Hasegawa, "Gait modification for improving walking stability of exoskeleton assisted paraplegic patient," *Robomech Journal*, vol. 7, no. 21, pp. 1–12, 2020.



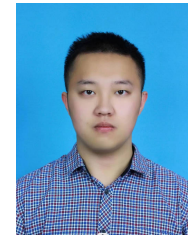
Chaobin Zou is a post-doctor from the Center for Robotics, School of Automation and Engineering, University of Electronic Science and Technology of China (UESTC), Chengdu, China. He received the Ph.D. degree in Control Science and Engineering in School of Automation Engineering, UESTC, in 2022. Dr. Zou has been a joint training doctoral student University of Hamburg from 2021 to 2022. His current research interests include motion planning, machine learning and optimization for robot control.



Zhihan Peng received the Ph.D. degree in Control Science and Engineering from the School of Automation Engineering, University of Electronic Science and Technology of China (UESTC) in 2020. From 2019 to 2020, Dr. Peng has been a joint training doctor with the University of Auckland. He is currently a Lecturer with the School of Automation Engineering, UESTC. His current research interests include multi-agent systems, adaptive dynamic programming, reinforcement learning and robot control.



Long Zhang received the B.E. degree from the University of Electronic Science and Technology of China (UESTC) in 2015. He received the Ph.D. degree in Control Science and Engineering in School of Automation and Engineering, UESTC, IN 2023. His current research interests include human-robot interaction and bionic control of legged robot, and focus on the lower limb exoskeleton robots.



Fengjun Mu received the B.E. degree in computer science and the M.S. degree in mechanical engineering from the University of Electronic Science and Technology of China, in 2019 and 2022. He is working toward the Ph.D. degree in control science and engineering from the University of Electronic Science and Technology of China. His research interests include Robot Perception, Computer Vision and Human-Robot Collaboration.



Rui Huang is an associate professor in School of Automation Engineering, University of Electronic Science and Technology of China (UESTC). He received Ph.D degree in Control Science and Engineering from UESTC in 2018. Dr. Huang has been a joint training doctoral student in TAMS, University of Hamburg from 2016 to 2017. His current research interests include reinforcement learning, exoskeleton robot, human-robot interaction and robot control.



Hong Cheng is a full Professor in School of Automation, a vice director of Center for Robotics, UESTC. He is the founding director of Machine Intelligence Institute, UESTC. He received Ph.D degree in Pattern Recognition and Intelligent Systems from Xi'an Jiaotong University in 2003. He was a postdoctoral at Computer Science School, Carnegie Mellon University, USA from 2006 to 2009. Since July 2000, he had been with Xi'an Jiaotong University, where he was a team leader of Intelligent Vehicle Group at the Institute of Artificial Intelligence and Robotics. His current research interests include computer vision, machine learning, robotics and human-robot interaction. Dr. Cheng has been a senior member of IEEE, ACM, and Associate Editor of IEEE Computational Intelligence Magazine. Dr. Cheng serves as Finance Chair of ICME 2014, Local arrangement chair of VLPR 2012, Registration Chair of the 2005 IEEE ICVES. He is a reviewer for many journals and conferences (IEEE TRO, TITS, CVPR, ICCV, ITSC, IVS, ACCV, ICRA, IROS, etc.).